Thermal Analysis of Friction in Coated Elastohydrodynamic Circular Contacts

W. Habchi*

Lebanese American University, Department of Industrial and Mechanical Engineering, Byblos, Lebanon

*Corresponding author: wassim.habchi@lau.edu.lb

Abstract

This paper presents a thermal analysis of friction in coated elastohydrodynamic contacts. In a previous work by the author, it was found that friction may be controlled in elastohydrodynamic contacts by a suitable choice of surface coatings based on thermal properties. Low thermal inertia coatings would reduce friction while high thermal inertia coatings would increase it. The current work attempts to investigate the origins of these observations by running a comprehensive thermal analysis of these contacts. It is also found that when both contacting surfaces are coated, friction is more influenced than when only one is coated. And in the latter case, under rolling-sliding conditions, friction is more affected when the faster moving surface is the coated one.

Keywords: Elastohydrodynamic Circular Contacts; Surface Coatings; Thermal Analysis; Finite Elements

1. Introduction

Surface coatings have been used for long to enhance the performance of dry contacts in rolling-sliding machine elements. The employed coatings were selected based on their mechanical properties to reduce the severity of a contact between two surfaces, leading to reduced friction and wear and thus enhanced fatigue life. Over the last few decades, the use of surface coatings has also extended to lubricated machine elements. The selection of these coatings was also largely based on the mechanical properties of their materials. For instance, smooth surface coatings with relatively small root-mean-square (rms) roughness can reduce friction in lubricated machine elements compared to their equivalent uncoated ones. Until recently, very little attention has been attributed to the thermal properties of coatings when it comes to their selection for lubricated machine elements under elastohydrodynamic lubrication (EHL) regime. However, recent experimental studies such as that of Evans et al. [1] or Kalin et al. [2] [3] have reported reduced friction in Diamond-Like- Carbon (DLC) coated EHL contacts. Originally, the reduced friction was attributed to boundary slip as a consequence of non-fully wetted surfaces. But for boundary slip to occur, surfaces have to be non or partially wetted by the lubricant, pressures must be low enough for the lubricant to be in its liquid form (as opposed to the glass state at high pressures) and the surfaces must be very smooth (below 6nm rms) [4]. Yet, Björling et al. [5] later reported in their experiments friction reduction under full-film regime with DLC coated surfaces even when the combined rms roughness of the surfaces was in the range of 155-355nm. This lead them to believe, based on a simplified analytical estimation of the

temperature increase in the lubricant film induced by the DLC surface coating, that the origins of the observed friction reduction might rather be thermal. This hypothesis found even more support when the authors validated their experimental results in [6] against numerical predictions of friction obtained using the full-system finite element approach [7] that does not incorporate any boundary slip effects. A detailed description of the employed numerical model was later provided in [8], in which the author showed that not only friction could be reduced by the use of low thermal inertia coatings (as is the case with DLC) but it can also be increased if high thermal inertia surface coatings are employed, and that in both cases lubricant film thickness is barely affected by the presence or absence of surface coatings. Thermal inertia I is actually a material property defined as $I = \sqrt{k\,\rho\,c} = \sqrt{k\,C}$, where C is the volumetric heat capacity of the material and k its thermal conductivity. And the terms "low" and "high" thermal inertia are relative to that of the substrate.

The current work attempts to analyze the origins of these friction variations in coated EHL contacts by means of a comprehensive analysis of their thermal behavior. In order to isolate the thermal influence of the employed coatings on the frictional behavior of the contact, only thin coatings with a thickness of t_c=2μm are considered. In fact, in [6] it was shown that for such relatively thin coatings, structural effects on the contacting solids were negligible while thermal effects prevailed. This simplifies the analysis (especially the elastic part and its associated computational cost) without removing the thermal effects to be investigated and their associated friction variations. Also note that in [8] it was shown that for such relatively thin coatings, the coating lies entirely within the thermal boundary layer of the solids. As a matter of fact, heat was shown to penetrate as deep as 80μm within the solids. As such, friction coefficients turned out to be no longer influenced beyond a coating thickness of 80μm. It is important to mention that friction in EHL contacts may also be significantly influenced by the surface finishing of the contacting elements as reported by Masjedi and Khonsari [9] in their simulation of rough EHL line contacts validated by experiments or also in the numerical simulations of Xu and Sadeghi [10] or the measurements of Björling et al. [11] for circular contacts. In fact, rough surfaces lead to higher friction coefficients than smooth ones under the same operating conditions. However, the influence of surface roughness on friction is beyond the scope of this work which aims at analyzing the effects of thermal properties of coatings on EHL friction. Therefore, only smooth surfaces are considered here.

2. Model description

The geometry of a circular EHD contact can be reduced to that of a contact between a plane and a ball of radius R as shown in Figure 1. A layer of coating is added to the surface of either the plane or the ball or both. It is assumed that the substrates of the two contacting bodies are made of the same material. As for coatings, they are assumed to be bonded to the substrates and both the substrates and coatings are considered to be perfectly elastic. The surfaces of the plane and ball are assumed to be smooth and moving at constant unidirectional surface speeds u_p and

u_b respectively in the x-direction. The contact is subject to an external applied load F and a fully-flooded regime is assumed. The lubricant is assumed to have a generalized-Newtonian behavior.

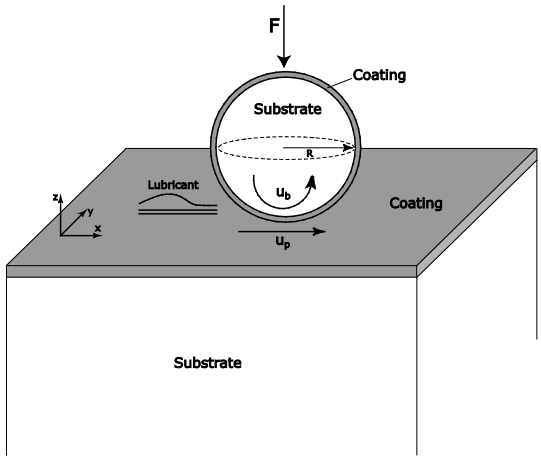

Figure 1: Geometry of the coated TEHD circular contact

The numerical model employed in this work has been described in detail in [8]. It consists in two distinct, yet coupled parts: the elastohydrodynamic part and the thermal part. Since the current work is focused on the thermal aspects of coated EHL contacts, only the details of the thermal model are reminded next, as for the EHD part the interested reader is referred to [8] for further details.

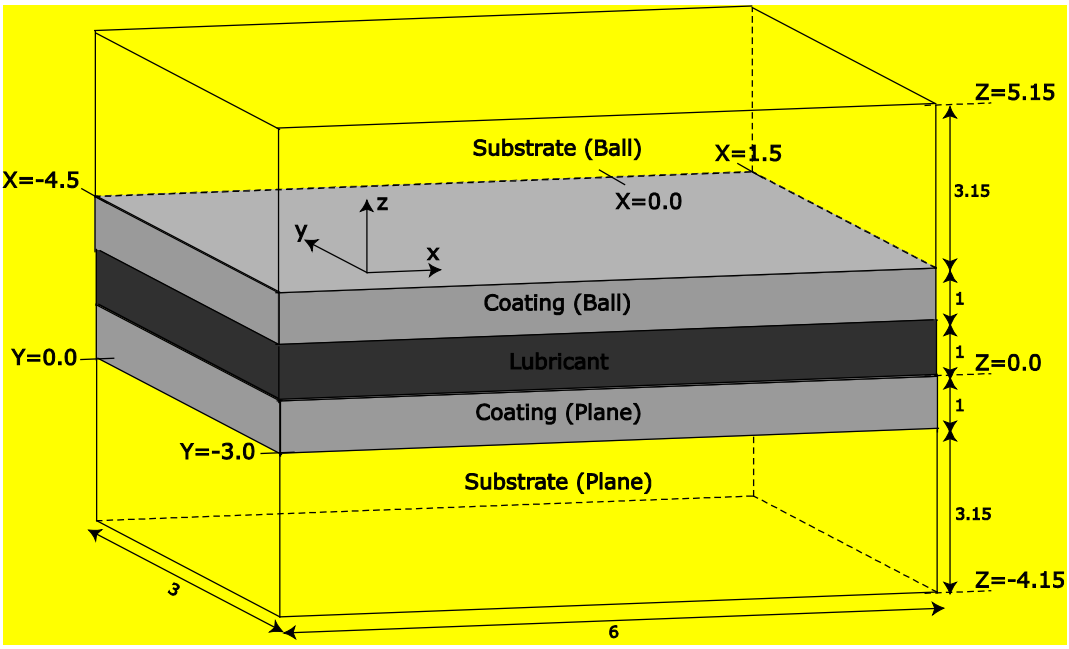

Figure 2: Computational domain of the thermal model for coated circular contacts

The geometrical domain for the thermal problem is shown in Figure 2 with the dimensionless space coordinates defined as follows:

$$X=\frac{x}{a},\ Y=\frac{y}{a},\ Z=\begin{cases} z/a & :\text{substrates} \\ z/t_c & :\text{coatings} \\ z/h & :\text{lubricant} \end{cases} \quad (1)$$

Note that the symmetry of the problem with respect to the *xz*-plane is taken into consideration to reduce the overall computational cost. Kaneta et al. [12] and Wang et al. [13] showed that for the contacting solids, in most cases, a dimensionless depth of 3.15 is sufficient to ensure a zero temperature gradient in regions far from the contact surface. Therefore, this depth is adopted for the substrates in the current work. The thermal part is based on the heat transfer equation applied to the lubricant and contacting solids:

$$\begin{cases} -\frac{\partial}{\partial X}\left(\frac{k_s}{a}\frac{\partial T}{\partial X}\right)-\frac{\partial}{\partial Y}\left(\frac{k_s}{a}\frac{\partial T}{\partial Y}\right)-\frac{\partial}{\partial Z}\left(\frac{k_s}{a}\frac{\partial T}{\partial Z}\right)+\rho_s c_s u_b\left(\frac{\partial T}{\partial X}\right)=0 & \text{(Ball Substrate)} \\ -\frac{\partial}{\partial X}\left(\frac{k_c t_c}{a^2}\frac{\partial T}{\partial X}\right)-\frac{\partial}{\partial Y}\left(\frac{k_c t_c}{a^2}\frac{\partial T}{\partial Y}\right)-\frac{\partial}{\partial Z}\left(\frac{k_c}{t_c}\frac{\partial T}{\partial Z}\right)+\rho_c c_c u_b\frac{t_c}{a}\left(\frac{\partial T}{\partial X}\right)=0 & \text{(Ball Coating)} \\ -\frac{\partial}{\partial Z}\left(\frac{kR}{Ha^2}\frac{\partial T}{\partial Z}\right)+\rho_R\bar{\rho}\,c\frac{Ha}{R}\left(u_f\frac{\partial T}{\partial X}+v_f\frac{\partial T}{\partial Y}\right)=Q_{comp}+Q_{shear} & \text{(Lubricant film)} \\ -\frac{\partial}{\partial X}\left(\frac{k_c t_c}{a^2}\frac{\partial T}{\partial X}\right)-\frac{\partial}{\partial Y}\left(\frac{k_c t_c}{a^2}\frac{\partial T}{\partial Y}\right)-\frac{\partial}{\partial Z}\left(\frac{k_c}{t_c}\frac{\partial T}{\partial Z}\right)+\rho_c c_c u_p\frac{t_c}{a}\left(\frac{\partial T}{\partial X}\right)=0 & \text{(Plane Coating)} \\ -\frac{\partial}{\partial X}\left(\frac{k_s}{a}\frac{\partial T}{\partial X}\right)-\frac{\partial}{\partial Y}\left(\frac{k_s}{a}\frac{\partial T}{\partial Y}\right)-\frac{\partial}{\partial Z}\left(\frac{k_s}{a}\frac{\partial T}{\partial Z}\right)+\rho_s c_s u_p\left(\frac{\partial T}{\partial X}\right)=0 & \text{(Plane Substrate)} \end{cases} \quad (2)$$

Where: $Q_{comp}=-\frac{T}{\bar{\rho}}\frac{\partial\bar{\rho}}{\partial T}p_h\frac{Ha}{R}\left(u_f\frac{\partial P}{\partial X}+v_f\frac{\partial P}{\partial Y}\right)$ and $Q_{shear}=\frac{\bar{\eta}\mu_R R}{Ha^2}\left[\left(\frac{\partial u_f}{\partial Z}\right)^2+\left(\frac{\partial v_f}{\partial Z}\right)^2\right]$

The terms Q_{comp} and Q_{shear} correspond to the compressive heating/cooling and shear heating source terms respectively while the terms u_f and v_f correspond to the lubricant velocity field components in the *x* and *y*-directions respectively. The transport properties as well as the thermal properties of the lubricant are allowed to vary with temperature and pressure across the lubricant film. The importance of accounting for the dependence of the thermal properties of the lubricant on temperature and pressure has been thoroughly discussed in [14] and [15]. In fact, it was shown that neglecting the variations of the lubricant's thermal properties with pressure and temperature leads to an underestimation of friction at high sliding speeds. To complete the thermal model, equations (2) are associated with the following boundary conditions:

$$\begin{cases} T\left(X=-4.5,Y,-4.15\le Z\le 0.0\right)=T\left(X=-4.5,Y,1.0\le Z\le 5.15\right)=T_0 \\ T\left(X,Y,Z=-4.15\right)=T\left(X,Y,Z=5.15\right)=T_0 \\ T\left(X=-4.5,Y,0.0\le Z\le 1.0\right)=T_0 \quad \text{where} \quad u_f\ge 0 \end{cases} \quad (3)$$

Note that boundary conditions are only required at inlet boundaries due to the hyperbolic nature of equations (2). Also note that zero heat flux (symmetry) boundary conditions are applied to the symmetry plane *xz* and heat flux continuity boundary conditions are imposed at all coating-lubricant and substrate-coating interfaces (as coatings are assumed to be perfectly bonded to the substrates). Equations (1)-(3) define the thermal part of the TEHL model for coated circular contacts. The finite element method is employed to discretize these equations using Lagrange second order tetrahedral elements.

The overall employed numerical model is based on the full-system finite element approach described in [7]. It consists in solving the thermal elastohydrodynamic (TEHD) lubrication problem in a fully-coupled way. The starting point is the selection of a suitable initial guess for the dimensionless pressure (P), dimensionless film thickness (H) and temperature (T) profiles. These are usually the dimensionless Hertzian pressure profile, its corresponding dimensionless film thickness profile and a homogeneous ambient temperature distribution ($T=T_0$) respectively. Assuming a fixed temperature distribution based on the initial guess, the generalized Reynolds equation [16], the linear elasticity equations and the load balance equation (EHL problem) are solved simultaneously using a Newton-like procedure. The simultaneous resolution of these equations avoids any loss of information that might arise in a weak coupling procedure (or semi-system approach) and leads to fast convergence rates. The solution of the EHL problem gives rise to new pressure and film thickness profiles that are then assumed to be fixed in solving the heat equations (thermal problem) in the lubricant and contacting solids (substrates and coatings) also using a Newton-like procedure. This gives rise to a new temperature profile, used in updating the initial guess. An iterative process is established between the respective solutions of the EHL and thermal problems (as shown in Figure 3) until convergence is attained. At every iteration, the initial guesses for P, H and T are updated to their respective solutions at the previous iteration

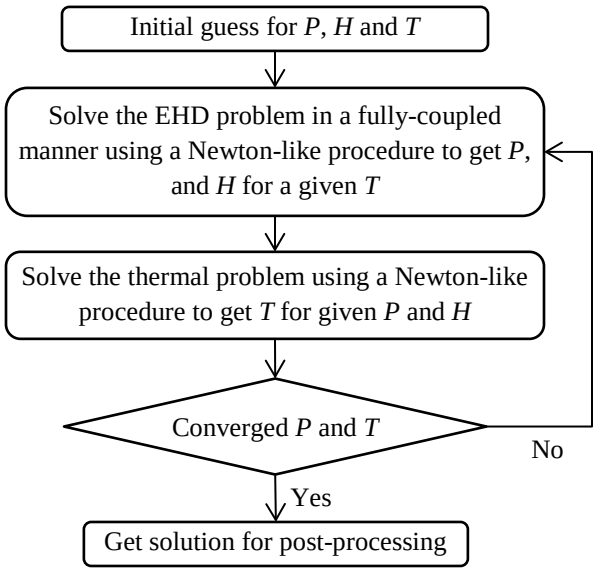

Figure 3: Flow chart of the overall iterative numerical procedure

Note that in the current work, since only thin coatings are considered; as mentioned earlier, their structural effect on the EHD part of the problem is negligible. Therefore, coatings are removed from the geometry of the solid components in the EHD part of the problem while these are kept for the thermal part. This leads to a significant reduction in the computational costs. Further reductions in computational costs are attained by taking advantage of the symmetry of the problem with respect to the *xz*-plane and solving the entire problem on half of the geometrical domain while the solution on the other half is deduced by symmetry.

Three different configurations will be considered throughout this work:

1. Uncoated (U): both surfaces are not coated.
2. One coated surface (C1): only one surface is coated, that of the ball.
3. Two coated surfaces (C2): both surfaces are coated.

The geometry of the thermal problem is not changed between configurations. Only the thermal properties of the geometrical domains are changed. In fact, for the uncoated case, the thermal properties of the coating domains of both the ball and the plane are taken to be similar to those of the substrate. As for the one coated surface case (1C), only the thermal properties of the plane's coating domain are taken to be similar to those of the substrate. For further details about the numerical model employed in this work, the interested reader is referred to [8].

3. Results

The lubricant selected for this work is Shell T9, a mineral oil for which the transport and thermal properties have been thoroughly characterized in [14] and fitted to appropriate mathematical models. In addition, in [14] numerical predictions of friction in TEHD contacts using this fluid have been validated against experiments. Note that the employed rheological models are strictly based on the actual measured transport properties of the mineral oil without any alteration of their corresponding parameters to force the agreement with friction measurements (an approach often employed by the EHL community). The rheological models represent the pressure, temperature, and shear stress dependence of viscosity including the limiting-shear-stress (LSS) behavior, in addition to the pressure-temperature dependence of the density and the thermal properties (thermal conductivity and heat capacity). An excellent agreement was obtained between experiments and numerical predictions giving rise to a legitimate and validated framework for the theoretical prediction of friction in EHL contacts. This work highlighted the importance of accounting for the dependence of lubricant's thermal properties on pressure and temperature when it comes to friction calculations [14]. In fact, it showed that neglecting this dependence can lead to an underestimation of friction coefficients under rolling-sliding conditions.

The different rheological models employed in describing the dependence of the lubricant's transport and thermal properties on pressure, temperature and shear stress are as follows. Subscripts *0* and *R* indicate, respectively, ambient pressure and temperature (p_0 = 0 and

$T_0 = 30^o\text{C}$) and a reference state ($p_R = 0$ and $T_R = 25^o\text{C}$). The lubricant's density variations with pressure and temperature are described by the Murnaghan [17] equation of state:

$$\rho = \frac{\rho_R}{1 + a_V\left(T - T_R\right)} \times \left(1 + \frac{K_0'}{K_0}\, p\right)^{\frac{1}{K_0'}} \quad \text{with} \quad K_0 = K_{00} \exp\left(-\beta_K T\right) \qquad (4)$$

Where $K_0' = 10.545$, $a_V = 7.734 \times 10^{-4}\ \text{K}^{-1}$, $K_{00} = 9.234\ \text{GPa}$, $\rho_R = 875\, Kg/m^3$ and $\beta_K = 6.090 \times 10^{-3}\ \text{K}^{-1}$. The low-shear viscosity dependence on temperature and pressure is described by a Vogel-like model [18][19]:

$$\mu = \mu_\infty \exp\left(\frac{B_F \varphi_\infty}{\varphi - \varphi_\infty}\right) \quad \text{with} \quad \varphi = \left(\frac{T}{T_R}\right)\left(\frac{V}{V_R}\right)^g \qquad (5)$$

Where $g = 5.0348$, $\varphi_\infty = 0.26844$, $B_F = 12.898$, and $\mu_\infty = 1.489 \times 10^{-4}\ \text{Pa}\cdot\text{s}$. And from the Murnaghan equation of state:

$$\frac{V}{V_R} = \frac{1 + a_V\left(T - T_R\right)}{\left(1 + \frac{K_0'}{K_0}\, p\right)^{1/K_0'}} \qquad (6)$$

Note that the low-shear viscosity at the reference state $\mu_R = 0.0135\ \text{Pa.s}$. For the shear dependence of viscosity, the single-Newtonian modified Carreau-Yasuda equation [20] is used to describe the dependence of the generalized viscosity η on shear stress τ:

$$\eta = \frac{\mu}{\left[1 + \left(\frac{\tau}{G}\right)^a\right]^{\frac{\frac{1}{n} - 1}{a}}} \qquad (7)$$

Where $G = 7.0\ \text{MPa}$, $a = 5$ and $n = 0.35$. As for the limiting-shear-stress τ_L, it is expressed as a function of pressure as follows:

$$\tau_L = \Lambda\ p \qquad (8)$$

Where the limiting stress-pressure coefficient $\Lambda = 0.083$ was deduced from EHL traction experiments carried out under isothermal operating conditions as detailed in [14]. The dependence of the thermal conductivity *k* of the lubricant on pressure and temperature is given by the following relationship [14]:

$$k = B_k + C_k \kappa^{-s} \quad \text{with} \quad \kappa = \left(\frac{V}{V_R}\right)\left[1 + A\left(\frac{T}{T_R}\right)\left(\frac{V}{V_R}\right)^3\right] \qquad (9)$$

Where $A = -0.101$, $B_k = 0.053\ \mathrm{W/m \cdot K}$, $C_k = 0.026\ \mathrm{W/m \cdot K}$ and $s = 7.6$. And finally, the dependence of the volumetric heat capacity C on pressure and temperature is given by the following relationship [14]:

$$C = C' + m\chi \qquad \text{with} \qquad \chi = \left(\frac{T}{T_R}\right)\left(\frac{V}{V_R}\right)^{-4} \qquad (10)$$

Where $C' = 1.17 \times 10^6\ J/m^3 \cdot K$ and $m = 0.39 \times 10^6\ \mathrm{J/m^3 \cdot K}$. The operating conditions selected for this work and the solid material properties are listed in Table 1. Note that a relatively low external applied load F=15N with a corresponding Hertzian contact pressure p_h=0.62GPa is selected. This is to avoid reaching the friction "Plateau regime" [21] in which the frictional behavior of the contact is governed by the LSS of the lubricant which smears out all other effects including generalized-Newtonian and thermal effects. The mean entrainment speed $u_m = (u_b + u_p)/2$ is taken to be u_m=1m/s. The corresponding values of the Moes [22] dimensionless parameters are M = 76 and L = 7 respectively. The slide-to-roll ratio $SRR = (u_b - u_p)/u_m$ is varied from -75% to +75%. A negative SRR value implies a faster moving plane whereas a positive value implies a faster moving ball. Note that the mechanical properties of the coatings (Young's modulus E_c and Poisson's coefficient υ_c) are not listed in Table 1 as these are not needed since only thin coatings are considered (t_c=2μm). In fact, as mentioned earlier, such thin coatings have a negligible structural effect on the solution of the EHD part of the problem and as a consequence they were removed from this part of the model. As for the thermal properties of the coatings, two types of coatings are considered; those with a lower thermal inertia than the substrate and those with a higher thermal inertia. Their corresponding densities, thermal conductivities and heat capacities are listed in Table 1.

Operating conditions	Solid material properties		
T_0=30°C	Substrate	Coatings	
u_m=1m/s	E_s=210GPa	Low thermal inertia	High thermal inertia
SRR=[-0.75 , 0.75]	υ_s=0.3	ρ_c=3500kg/m^3	ρ_c=10000kg/m^3
F=15N	ρ_s=7850kg/m^3	k_c=5W/m.K	k_c=90W/m.K
R=12.7mm	k_s=46W/m.K	c_c=200J/kg.K	c_c=1000J/kg.K
t_c=2μm	c_s=470J/kg.K		

Table 1: Operating conditions and solid material properties

Figure 4 shows the friction curves under the load and speed conditions considered here for the uncoated ball and plane case (U), the coated ball case (C1) and the coated ball and plane case (C2). Both high and low inertia coatings are considered for the C1 and C2 cases. The following observations can be drawn from this figure:

1- High thermal inertia coatings lead to increased friction while low thermal inertia coatings lead to reduced friction as was stated in [8].

2- When both surfaces are coated (C2) friction is more affected than in the case of only a coated ball (C1). In fact, when both surfaces are coated with high thermal inertia coatings, friction

exhibits a more significant increase and when these are coated with low thermal inertia coatings it exhibits a more significant decrease. This last statement confirms the experimental observations of Björling et al. [5] for steel surfaces with DLC coatings. In fact, DLC has a lower thermal inertia than steel and in [5] the authors noted a more significant friction reduction when both surfaces are coated compared to the case where only one surface is coated.

3- When only one surface is coated (C1), friction is more affected if the coated surface is the faster moving one. In fact, for the uncoated case (U) and the case of two coated surfaces (C2), friction curves are perfectly symmetric with respect to the origin. However, though this is barely noticeable on the figure, for the case of one coated surface (C1), this symmetry is lost. In fact, with the high thermal inertia coating the friction coefficient in absolute value at SRR=-0.75 is 0.0594 (plane moving faster) while at SRR=+0.75 it is 0.0597 (ball moving faster). Compared to the uncoated case where the friction coefficient in absolute value is 0.0591 for both SRR=-0.75 and SRR=+0.75, it is clear that when the coated surface (ball) is moving faster, friction exhibits a more important variation (increase). As for the case with the low thermal inertia coating, the friction coefficient in absolute value at SRR=-0.75 is 0.0572 (plane moving faster) while at SRR=+0.75 it is 0.0564 (ball moving faster). Again, compared to the uncoated case, when the coated surface (ball) is moving faster, friction exhibits a more important variation (decrease).

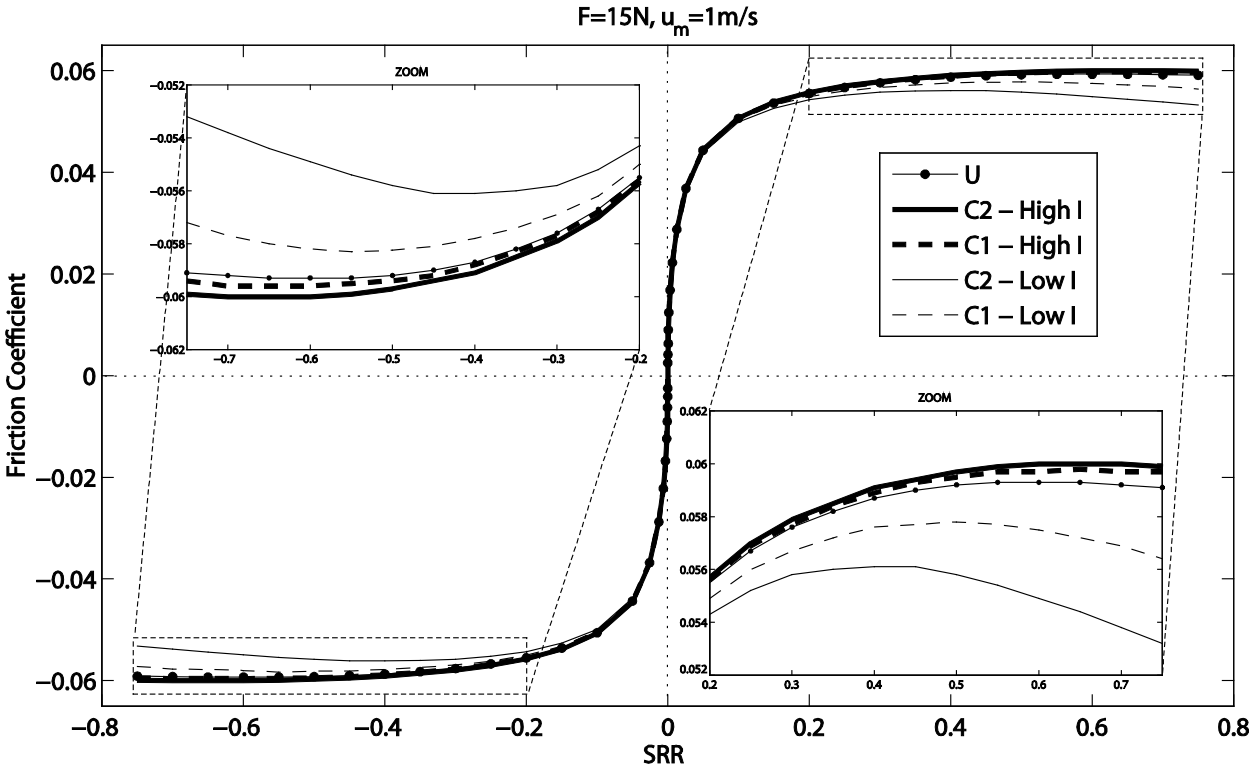

Figure 4: Friction curves for the case F=15N, u_m=1m/s with uncoated ball and plane (U), coated ball (C1) and coated ball and plane (C2)

The origins of these observations are investigated next by carefully examining the localized thermal behavior of the contact.

4. Discussion

Before moving to a thorough thermal analysis of coated TEHD contacts, first it is essential to understand the concepts of heat generation and heat removal in any EHD contact (coated or uncoated).

4.1. Heat generation and removal in EHD contacts

The concepts of heat generation and removal in elastohydrodynamic lubricated contacts are illustrated in figure 5. Heat is generated in an EHL conjunction by two separate mechanisms: compression and shear. The former is associated with the lubricant compression towards the inlet region of the contact. In fact, when compressed, any fluid would generate heat. However, in an EHL contact the lubricant is compressed on the inlet side of the contact (left side of figure 5), but then as it heads towards the outlet (right side) it is expanded. Therefore, a cooling effect is observed towards the outlet of the contact. This heating/cooling mechanism due to compression/expansion generally has a negligible effect especially compared to shear heating. In fact, compression heating/cooling is only significant under pure-rolling conditions in the absence of any significant shear effects. Under rolling-sliding conditions, heat is also generated in the lubricant film by shear. Given the relatively small lubricant film thickness at the center of the contact and its high viscosity (owing to high pressure), the amount of heat generated in the central part of the contact by shear can be several orders of magnitude greater than the amount generated by compression. In the inlet of the contact, given the relatively larger lubricant film thickness, the amount of heat generated by shear remains small. This being said, the bulk of heat generation in an EHL conjunction occurs in the central part of the contact.

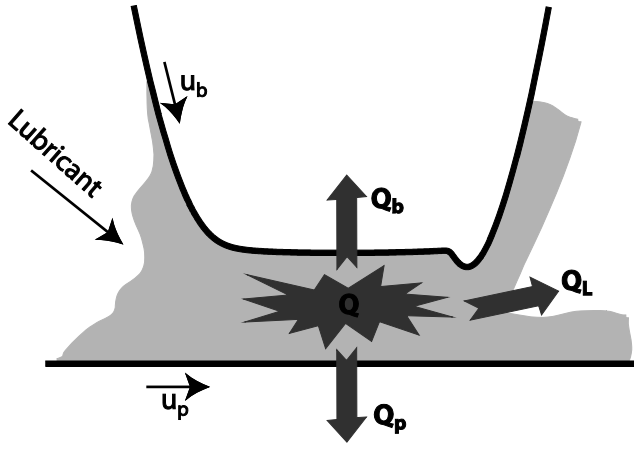

Figure 5: Heat transfer in an EHL contact

The heat generated within the lubricant film is removed from the contact by two separate mechanisms. First, part of the generated heat is transferred to the contacting solids by conduction. This part is then carried away by the moving solids towards the outlet of the contact by advection (heat transfer by mass) where it is released to the environment which is usually at a

relatively lower temperature T_0 (provided enough time is allowed for the solid's surface to cool down and reach T_0 before it passes through the contact again). The other mechanism of heat removal from the contact region is conduction and advection within the lubricant film itself. In fact, the moving lubricant carries away a significant portion of the heat generated inside the conjunction towards the exit of the contact by advection and towards the peripheral area (inlet, outlet and sides) of the contact by conduction. Obviously, the proportion of heat removed by the solids and by the lubricant depends on their respective thermal properties. The same can be said about the proportion of heat removed by advection compared to that removed by conduction within the solids or the lubricant film. To better understand this point, a discussion on the role of different thermal properties of a material when it comes to heat removal is needed. In fact, heat transfer by conduction within a given material is dictated by its thermal conductivity k whereas its volumetric heat capacity $C = \rho c$ (ρ: density; c: specific heat) represents its ability to store and transport heat by advection. The amount of heat removed by advection also depends on the speed of the medium, but speed is not a property of the material. This being said, thermal inertia $I = \sqrt{k \rho c} = \sqrt{k C}$ represents the ability of a material to transport heat by both conduction and advection. In fact, a high thermal inertia material usually has a high thermal conductivity and volumetric heat capacity. As such, it has a high ability to transport heat by conduction and advection respectively. On the other hand, a low thermal inertia material has a low ability to transport heat by conduction and advection, and thus it acts as an insulating material.

4.2. Origins of friction variations in coated EHD contacts

Now the ground is well set for investigating the origins of the different observations made in section 3. Figure 6 shows the temperature distribution in the mid-plane of the lubricant film along the central line of the contact in the x-direction for the case SRR=+0.75. Note that high thermal inertia coatings generally lead to lower temperatures within the lubricant film while low thermal inertia coatings lead to higher temperatures. This is to be expected since a high thermal inertia coating implies a more important heat removal both by conduction and advection, while a low thermal inertia coating implies a less important heat removal. Therefore, since lower lubricant film temperatures are observed with high thermal inertia coatings, this would lead to higher lubricant viscosities and thus higher friction. The opposite holds with low thermal inertia coatings leading to lower friction coefficients. This explains the first observation made in the section 3.

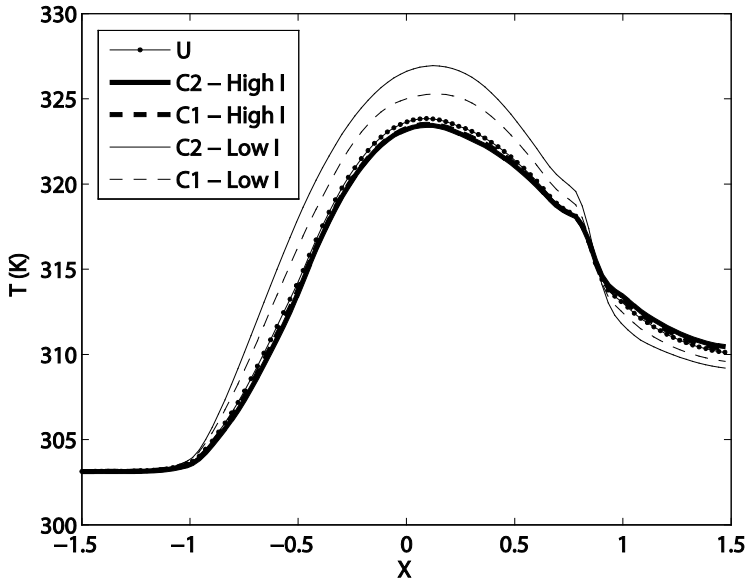

Figure 6: Temperature distribution in the mid-plane of the lubricant film along the central line in the *x*-direction for the case SRR=+0.75

On the other hand, note that the temperature increase for low thermal inertia coatings or temperature decrease for high thermal inertia coatings compared to the uncoated case is more pronounced when both contacting surfaces are coated (compared to the case of a coated ball only). In fact, the temperature increase with respect to the uncoated case for the case "C2 - Low I" is more important than for the case "C1 - Low I" leading to lower viscosities and thus lower friction coefficients in the former case. Similarly, the temperature decrease with respect to the uncoated case for the case "C2 - High I" is more important than for the case "C1 - High I" leading to higher viscosities and thus higher friction coefficients in the former case. This explains the second observation made in section 3 and the experimental observations of Björling et al. [5].

Also note that the temperature trends in figure 6 are inverted towards the contact's exit. That is, lubricant's temperature becomes higher with higher thermal inertia coatings and lower with lower thermal inertia coatings. In [8], the author suggested that this is a result of heat transfer by conduction and advection within the coating from the center of the contact (where most of the heat is generated) towards the outlet. In fact, high thermal inertia coatings can transport more heat towards the contact's exit which leads to higher solid surface temperatures there, maintaining the lubricant film at a higher temperature. This is confirmed by a careful examination of the heat fluxes going through the ball's surface (Q_b) and the plane's surface (Q_p) by conduction as reported in Table 2 for the cases SRR=-0.75 and SRR=+0.75 for all considered configurations. Obviously, more heat passes through a solid-lubricant interface when the solid surface is coated with a high inertia coating and less heat goes through when the coating is of lower thermal inertia than the substrate. And this effect is more emphasized when both surfaces are coated compared to the case of a coated ball only. Note that the amount of heat generated within the lubricant film ($Traction\ Force \times Sliding\ Speed$) is roughly the same in all considered

cases ($\approx 0.65\,W$) as the operating conditions are the same and the lubricant film thickness is barely affected by the presence or absence of surface coatings as reported in [8]. In fact, lubricant film thickness in EHD contacts is known to be governed by hydrodynamic effects in the inlet region of the contact. But, by examining the temperature profiles provided in figure 6, it is clear that in the inlet region of the contact, temperature is roughly the same for all considered configurations, leading to similar viscosities and thus similar film thicknesses. In fact, the central and minimum film thicknesses for the case considered here are 140nm and 76nm respectively and in the most extreme cases ($SRR = \pm 0.75$) the maximum deviation in central film thickness between different configurations remains less than 2.5% while for minimum film thickness it is less than 0.5%.

	SRR = - 0.75			SRR = + 0.75		
	Q_b (W)	Q_p (W)	Q_b+Q_p (W)	Q_b (W)	Q_p (W)	Q_b+Q_p (W)
U	0.134	0.175	0.309	0.175	0.134	0.309
C2 – High I	0.138	0.184	0.322	0.184	0.138	0.322
C1 – High I	0.139	0.176	0.315	0.184	0.133	0.317
C2 – Low I	0.118	0.148	0.266	0.148	0.118	0.266
C1 – Low I	0.111	0.176	0.287	0.145	0.140	0.285

Table 2: Conduction heat fluxes from the lubricant film through the ball's surface Q_b and plane's surface Q_p for SRR=-0.75 and SRR=+0.75

Figure 7 shows the maximum temperature increase within the lubricant film as a function of the slide-to-roll ratio. It is clear that deviations in temperature between the different considered configurations only become significant at values of SRR exceeding 0.2 in absolute value. This is why the friction curves in figure 4 only deviate beyond this value of SRR.

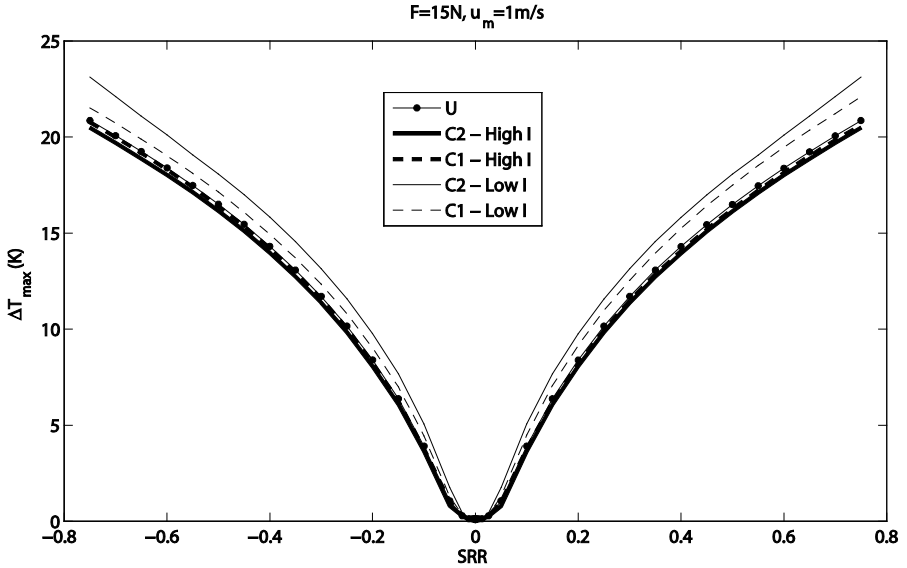

Figure 7: Maximum temperature increase in the lubricant film as a function of SRR

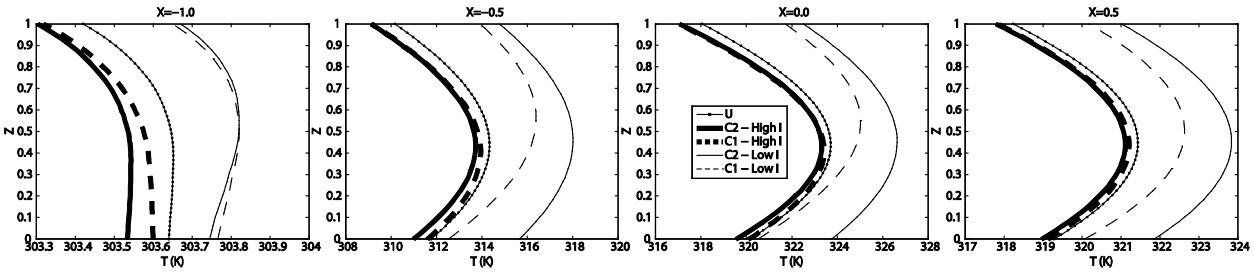

Figure 8: Temperature distribution across the lubricant film thickness at different locations along the central line in the *x*-direction for the case SRR=+0.75

Figure 8 shows the temperature distribution across the lubricant film thickness at different locations along the central line in the *x*-direction for the case SRR=+0.75. Note that $X = x/a$ where a is the Hertzian contact radius. Thus X=-1.0 corresponds to the border of the Hertzian contact region on the inlet side and X=0.0 corresponds to the center of the Hertzian contact. Also note that $Z = z/h$ where h is the lubricant film thickness with Z=0 corresponding to the plane's surface while Z=1 corresponds to the ball's surface. By carefully examining figure 8, many interesting observations can be revealed. First, it confirms that high thermal inertia coatings generally lead to lower lubricant temperatures and low thermal inertia coatings lead to higher lubricant temperatures and that this effect is more pronounced when both contacting surfaces are coated than when only the ball is coated. Second, note that under all configurations the plane's surface temperature is higher than that of the ball except for the "C1 – Low I" case. Remember that for positive SRR values (as is the case here), the ball is moving faster than the plane. This means that the ball can transport more heat away from the contact by advection. However, heat must reach the ball first by conduction within the lubricant film and through the surface coating (if the ball is coated). In the U and C2 cases, both the ball and plane have similar thermal properties so they would remove the same amount of heat from the lubricant film by conduction. But since the ball is moving faster, it would transport more of this heat away from the contact by advection, which explains the ball's lower surface temperature. For the case "C1 – High I" the ball is coated with a high thermal inertia material which increases its heat removal capability, and in addition, since it is moving at a higher speed, this also leads to enhanced heat removal by advection leading also to a lower surface temperature than that of the plane. However, in the "C1 – Low I" case, the ball is now coated with a low thermal inertia coating which acts as an insulator preventing heat from actually reaching the substrate and being removed by advection. And in the current case, even though the plane is moving slower, it is capable of an overall more important heat removal by conduction and advection leading to its lower surface temperature compared to that of the ball. This is partially confirmed by examining the values of Q_b and Q_p in the last row of table 2 for SRR=+0.75 which only reflect the conductive heat fluxes through the ball's and plane's surface respectively. In fact, for all considered configurations Q_b is significantly larger than Q_p except for the "C1 – Low I" case where the difference becomes much smaller (though Q_b remains larger). This is only a partial confirmation since Q_b and Q_p only represent part of the heat removal from the contact region and not all of it. In fact, there is also the heat removed by conduction and advection within the lubricant film itself Q_L.

Obviously, the plane's surface temperature in the "C1 – Low I" case will not always be lower than that of the ball's surface irrespective of the SRR. In fact, if the SRR were to be further increased, a point would be reached where the plane's surface speed would be too small such that even if the ball is coated with a low thermal inertia coating and very little heat reaches the substrate, it is moving so fast that all this heat would be continuously removed by advection and an overall more significant heat removal would be attained leading to a lower surface temperature compared to that of the plane.

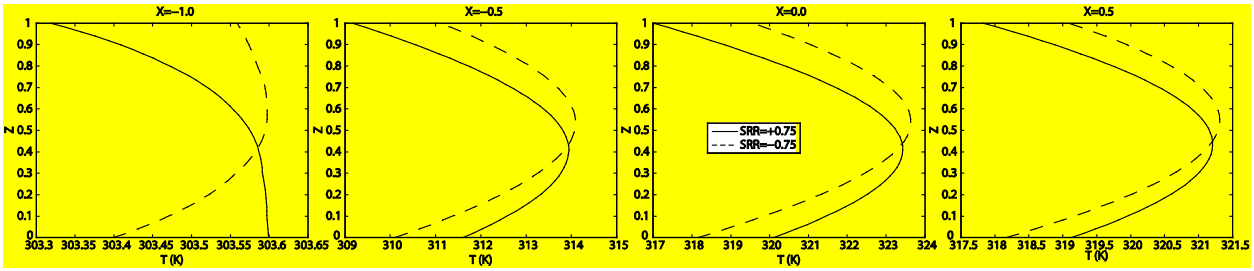

Figure 9: Comparison of temperature distributions for the case C1 (High I) across the lubricant film thickness for SRR=+0.75 and SRR=-0.75 at different locations along the central line in the *x*-direction

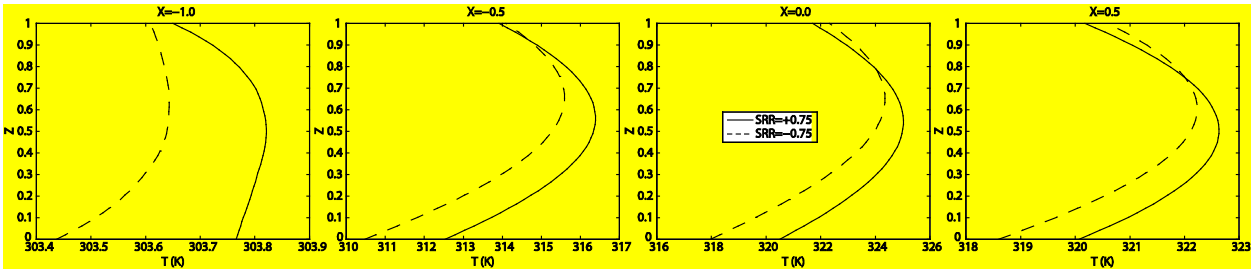

Figure 10: Comparison of temperature distributions for the case C1 (Low I) across the lubricant film thickness for SRR=+0.75 and SRR=-0.75 at different locations along the central line in the *x*-direction

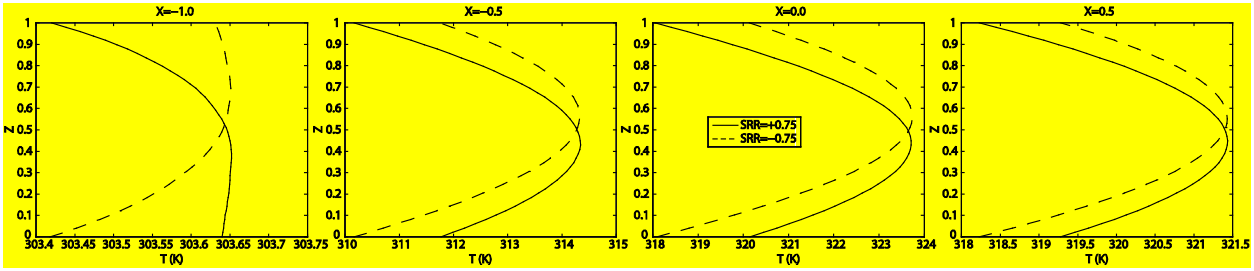

Figure 11: Comparison of temperature distributions for the case U across the lubricant film thickness for SRR=+0.75 and SRR=-0.75 at different locations along the central line in the *x*-direction

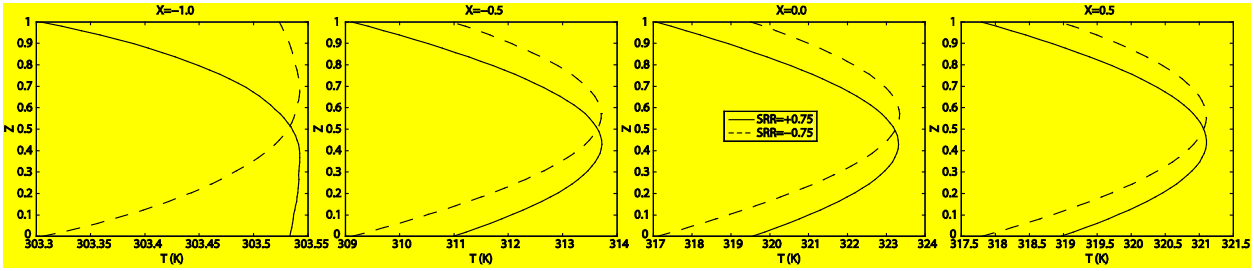

Figure 12: Comparison of temperature distributions for the case C2 (High I) across the lubricant film thickness for SRR=+0.75 and SRR=-0.75 at different locations along the central line in the *x*-direction

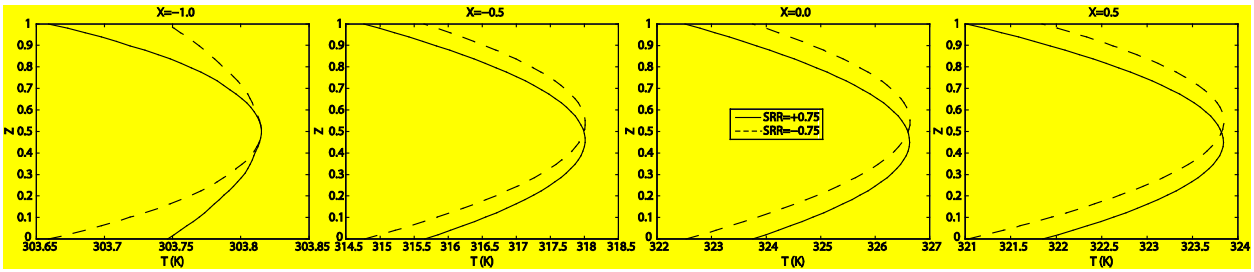

Figure 13: Comparison of temperature distributions for the case C2 (Low I) across the lubricant film thickness for SRR=+0.75 and SRR=-0.75 at different locations along the central line in the *x*-direction

So far, the discussion in this section has managed to provide an explanation for the first two observations made in section 3. That is, it has explained why low thermal inertia coatings lead to reduced friction in coated TEHD contacts while high thermal inertia coatings lead to increased friction and why both effects are more pronounced when both contacting surfaces are coated compared to the case where only one is coated. It remains to explain why when only one surface is coated; friction is more affected if the coated surface is the faster moving one. For this, let us start by examining figure 9 which provides a comparison of temperature distributions across the lubricant film thickness for the case "C1 – High I" for SRR=+0.75 and SRR=-0.75 at different locations along the central line in the *x*-direction. Remember that for the C1 cases, only the ball is coated and note that generally, the temperature within the lubricant film is slightly lower for SRR=+0.75; that is when the ball is moving faster than the plane. This leads to slightly higher viscosities and thus increased friction coefficients. This explains why friction increase with respect to the uncoated case is more important for positive SRR (ball moving faster) than it is for negative SRR (plane moving faster).

Similarly, examining figure 10 which provides temperature distributions across the lubricant film thickness for the case "C1 – Low I" for SRR=+0.75 and SRR=-0.75, it is clear that now temperature within the lubricant film is generally higher for SRR=+0.75 (ball moving faster). This leads to lower viscosities and thus reduced friction coefficients. This explains why friction reduction with respect to the uncoated case is more important for positive SRR (ball moving faster) than it is for negative SRR (plane moving faster).

For both cases "C1 – Low I" and "C1 – High I" the explanation is that if only one surface is to be coated to either reduce or increase friction respectively, it would better be the surface that contributes more to heat removal from the contact region; that is, the faster moving one since it removes more heat by advection (all other things being equal). In fact, if the goal is to increase friction; by coating the faster moving surface with a high thermal inertia coating, a higher heat flux would go through it by conduction allowing it to transport even more heat by advection. On the other hand, if the goal is to reduce friction; by coating the faster moving surface with a low thermal inertia coating, it would act as an insulator, preventing what used to be the larger heat flux from going through by conduction to reach the substrate and thus preventing its transport by advection within the solid that contributes the most to advection.

Finally, note that temperature profiles for positive and negative SRR within the lubricant film thickness for the cases “C1 – Low I” and “C1 – High I” are not symmetric with respect to the mid-plane (Z=0.5). This is because coating only one surface makes the geometry of the problem loose its symmetry with respect to the mid-plane of the lubricant film. The temperature profiles for the cases “U”, “C2 – High I” and “C2 – Low I” are provided in figures 11, 12 and 13 respectively. Obviously, the profiles for SRR=+0.75 and SRR=-0.75 are in these cases perfectly symmetric with respect to the mid-plane of the lubricant film. This is because the geometry of the problem is now symmetric with respect to the mid-plane and only the surface speed conditions are inverted. For instance, for SRR=+0.75, u_b=1.375m/s and u_p=0.625m/s while for SRR=-0.75, u_b=0.625m/s and u_p=1.375m/s. This symmetry could also be observed for the friction curves of these cases (“U”, “C2 – High I” and “C2 – Low I”) in figure 4 with respect to the origin, while this symmetry is lost for the “C1 – Low I” and “C1 – High I” cases. The same can be said about the maximum temperature increase curves of figure 7 and their symmetry with respect to the ordinate axis or also the heat flux values reported in table 2. In fact, for the “U”, “C2 – High I” and “C2 – Low I” cases, Q_b(SRR=-0.75)=Q_p(SRR=+0.75) and Q_p(SRR=-0.75)=Q_b(SRR=+0.75) while this does not hold for the “C1 – Low I” and “C1 – High I” cases.

5. Conclusion

In this work, a thorough thermal analysis of friction in coated elastohydrodynamic contacts is presented, showing that friction may be controlled in EHD contacts by a suitable choice of surface coating based on thermal properties, without inducing any significant changes in lubricant film thickness. It is found that:

1- High thermal inertia coatings lead to increased friction while low thermal inertia coatings lead to reduced friction as was stated in [8].
2- When both surfaces are coated friction is more affected than in the case of only one coated surface.
3- When only one surface is coated, friction is more affected if the coated surface is the faster moving one.

The explanation for the first observation is that high thermal inertia coatings lead to enhanced heat removal from the contact towards its surroundings, leading to lower lubricant film temperatures and thus higher viscosities and increased friction. For low thermal inertia coatings, the opposite holds. That is, low thermal inertia coatings act as insulators, preventing heat removal by the substrates and confining the generated heat within the contact. This leads to higher lubricant film temperatures and as a consequence lower viscosities and reduced friction. This also provides an explanation to the second observation, as clearly, if two surfaces are coated, more heat would be removed from the contact than if only one is coated in the case of a high thermal inertia coating (or less heat in the case of a low thermal inertia coating). And finally, the explanation to the last observation is that if only one surface is to be coated to either reduce or increase friction respectively, it would better be the surface that contributes more to

heat removal from the contact region; that is, the faster moving one since it removes more heat by advection (all other things being equal).

Nomenclature

η : Lubricant's Generalized Newtonian viscosity (Pa.s)
μ : Lubricant's viscosity (Pa.s)
μ_R : Lubricant's viscosity at reference state (Pa.s)
μ_∞ : Lubricant's viscosity extrapolated to infinite temperature (Pa.s)
υ_c : Coating's Poisson coefficient
υ_s : Substrate's Poisson coefficient
Λ : Limiting stress-pressure coefficient
ρ : Lubricant's density (kg/m^3)
ρ_c : Coating's density (kg/m^3)
ρ_s : Substrate's density (kg/m^3)
ρ_R : Lubricant's density at reference state (kg/m^3)
τ : Shear stress (Pa)
τ_L : Limiting shear stress (Pa)
a : Hertzian contact radius (m)
c : Lubricant's heat capacity (J/kg.K)
c_c : Coating's heat capacity (J/kg.K)
c_s : Substrate's heat capacity (J/kg.K)
C : Lubricant's volumetric heat capacity (J/m^3.K)
E_c : Coating's Young's modulus of elasticity (Pa)
E_s : Substrate's Young's modulus of elasticity (Pa)
F : Contact external applied load (N)
G : Lubricant effective shear modulus (Pa)
h : Lubricant film thickness (m)
H : Dimensionless lubricant film thickness
k : Lubricant's thermal conductivity (W/m.K)
k_c : Coating's thermal conductivity (W/m.K)
k_s : Substrate's thermal conductivity (W/m.K)
p : Pressure (Pa)
P : Dimensionless pressure
p_h : Hertzian contact pressure (Pa)
p_0 : Ambient pressure (Pa)
p_R : Reference pressure (Pa)
R : Ball's radius (m)
SRR : Slide-to-Roll ratio = $(u_b\text{-}u_p)/u_m$
t_c : Coating's thickness (m)
T : Temperature (°C)
T_0 : Ambient temperature (°C)

T_R : Reference temperature (°C)
u_m : Mean entrainment speed = $(u_b+u_p)/2$ (m/s)
u_b : Ball's surface velocity (m/s)
u_f, v_f : Lubricant's velocity field components in the x and y-directions (m/s)
u_p : Plane's surface velocity (m/s)
V : Volume (m^3)
V_R : Volume at reference state (m^3)
x, y, z : Space coordinates (m)
X, Y, Z : Dimensionless space coordinates

Subscripts

b : Ball
c : Coating
p : Plane
s : Substrate

References

[1] Evans R. D., Cogdell J. D., and Richter G. A. - Traction of Lubricated Rolling Contacts Between Thin-Film Coatings and Steel, *Tribology Transactions*, 2009, vol. 52 (1), pp. 106–113.

[2] Kalin M. and Polajnar, M. - The Correlation Between the Surface Energy, the Contact Angle and the Spreading Parameter, and their Relevance for the Wetting Behaviour of DLC with lubricating oils, *Tribology International*, 2013, vol. 66, pp. 225–233.

[3] Kalin M., Velkavrh I. and Vižintin J. - The Stribeck Curve and Lubrication Design for Non-Fully Wetted Surfaces, *Wear*, 2009, vol. 267 (5-8), pp. 1232–1240.

[4] Zhu Y. and Granick S. - Limits of the Hydrodynamic No-Slip Boundary Condition, *Physical Review Letters*, 2002, vol. 88 (10), 106102 (1-4).

[5] Björling M., Isaksson P., Marklund P. and Larsson R. – The Influence of DLC Coating on EHL Friction Coefficient, *Tribology Letters*, 2012, vol. 47, pp. 285-294.

[6] Björling M., Habchi W., Bair S., Larsson R. and Marklund P. - Friction Reduction in Elastohydrodynamic Contacts by Thin Layer Thermal Insulation, *Tribology Letters*, 2014, vol. 53, pp. 477-486.

[7] Habchi W., Eyheramendy D., Vergne P. and Morales-Espejel G. – Stabilized Fully-Coupled Finite Elements for Elastohydrodynamic Lubrication Problems, *Advances in Engineering Software*, 2012, vol. 46, pp. 4-18.

[8] Habchi W. – A Numerical Model for the Solution of Thermal Elastohydrodynamic Lubrication in Coated Circular Contacts, *Tribology International*, 2014, vol. 73, pp. 57-68.

[9] Masjedi M. and Khonsari M. - Theoretical and Experimental Investigation of Traction Coefficient in Line-Contact EHL of Rough Surfaces, *Tribology International*, 2014, vol. 70, pp. 179-189.

[10] Xu G. and Sadeghi F. - Thermal EHL Analysis of Circular Contacts with Measured Surface Roughness, *ASME Journal of Tribology*, 1996, vol. 118 (3), doi:10.1115/1.2831560.
[11] Björling M., Larsson R., Marklund P. and Kassfeldt E. - Elastohydrodynamic Lubrication Friction Mapping – The Influence of Lubricant, Roughness, Speed, and Slide-to-Roll Ratio, *IMEchE Part J, Journal of Engineering Tribology*, 2011, vol. 225, pp. 671-681.
[12] Kaneta M., Shigeta T. and Yang P. – Film Pressure Distributions in Point Contacts Predicted by Thermal EHL Analysis, *Tribology International*, 2006, vol. 39, pp. 812-819.
[13] Wang Y., Li H., Tong J. and Yang P. – Transient Thermoelastohydrodynamic Lubrication Analysis of an Involute Spur Gear, *Tribology International*, 2004, vol. 37, pp. 773-782.
[14] Habchi W., Vergne P., Bair S., Andersson O., Eyheramendy D. and Morales-Espejel G. E. – Influence of Pressure and Temperature Dependence of Thermal Properties of a Lubricant on the Behaviour of Circular TEHD Contacts, *Tribology International*, 2010, vol. 43, pp. 1842-1850.
[15] Habchi W., Vergne P., Fillot N., Bair S. and Morales-Espejel G. E. – A Numerical Investigation of Local Effects on the Global Behavior of TEHD Highly Loaded Circular Contacts, *Tribology International*, 2011, vol. 44, pp. 1987-1996.
[16] Yang P. and Wen S. - A Generalized Reynolds Equation for Non-Newtonian Thermal Elastohydrodynamic Lubrication, *ASME Journal of Tribology*, 1990, vol. 112, pp. 631-636.
[17] Murnaghan F. D. - The Compressibility of Media under Extreme Pressures, *Proceedings of the National Academy of Sciences*, 1944, vol. 30, p. 244-247.
[18] Vogel H. – The Temperature Dependence Law of the Viscosity of Fluids, *Physikalische Zeitschrift*, 1921, vol. 22, pp. 645-646.
[19] Bair S. – High Pressure Rheology for Quantitative Elastohydrodynamics, Elsevier Science, Amsterdam, 2007.
[20] Bair S. - A Rough Shear Thinning Correction for EHD Film Thickness, *STLE Tribology Trans.*, 2004, vol. 47, pp. 361-365.
[21] Habchi W., Bair S. and Vergne P. – On Friction Regimes in Quantitative Elastohydrodynamics, *Tribology International*, 2013, vol. 58, pp. 107-117.
[22] Moes H. – Optimum Similarity Analysis with Applications to Elastohydrodynamic Lubrication, *Wear*, 1992, vol. 159, pp. 57-66.